Wind Energy Conversion System with Integrated Power Smoothing Capability based on an EVT-coupled Flywheel

MARCELO G. CENDOYA, SANTIAGO A. VERNE, MARÍA I. VALLA,
PEDRO E. BATTAIOTTO
Instituto de Investigaciones en Electrónica, Control y Procesamiento de Señales (LEICI),
UNLP - CONICET - CIC PBA,
Departamento de Electrotecnia, Facultad de Ingeniería,
Universidad Nacional de La Plata,
Calle 1 y 47, La Plata (B1900TAG), Buenos Aires,
ARGENTINA

Abstract: - This paper presents a wind energy conversion system that integrates, in a compact form, both generation and power smoothing functions. The system is based on a vertical axis wind turbine (VAWT) and a low-speed flywheel that are coupled by an electric variable transmission (EVT). The EVT performs a dual function by simultaneously injecting power to the grid and regulating the power flow to the flywheel to smooth the power fluctuation caused by wind turbulences. The main advantages of the presented generation/smoothing topology are integrating two machines (generator and motor) in the same physical structure and the reduced power demanded by the converter that feeds the flywheel's rotor. A theoretical analysis is carried out to determine an appropriate control law and flywheel sizing to satisfy a desired attenuation of the power fluctuation. Simulation results show an effective smoothing action, as the power fluctuation is reduced to an adequate level. In addition, the validity of the flywheel sizing procedure is verified.

Keywords: - Vertical Axis Wind Turbines; Power Smoothing; Wind Turbulence; Low-speed Flywheel; Electric Variable Transmission; Weak Grid; Renewable Distributed Generation; Wind Energy Conversion.

Received: March 11, 2023. Revised: December 19, 2023. Accepted: February 7, 2024. Published: March 27, 2024.

1 Introduction

The southern region of Argentina, widely known as "Patagonia," has several remote villages dedicated to agricultural, livestock, mining, and oil activities. As is well known, the availability of abundant electrical energy is a key driver for the development and growth of such productions. While numerous rural settlements have access to electricity grids, these lines are typically weak and can only provide a limited amount of power to meet current demand. Moreover, due to their low population, renewal or expansion of these grids is unlikely to occur, as the energy distribution companies would need to absorb the high costs involved with little economic return. Fortunately, this region of the country has significant wind energy potential, [1], [2], which has led to numerous wind farm projects. However, these farms, typically of large energy production, are designed to supply major power consumption centers rather than small rural villages. As a result, to increase the available electrical power, inhabitants of these villages must individually turn to the utilization of diesel generators. This entails undesirable environmental pollution and high operating costs, as the elevated fuel prices are compounded by the cost of transportation from remote locations. This scenario motivates the search for alternative solutions, and in this context, the application of Renewable Distributed Generation (RDG) seems appropriate, [3]. In RDG, small-scale generation close to consumption points replaces large and distant generation plants, eliminating the need for long and expensive transmission lines and associated equipment.

Due to its remarkable characteristics in terms of high energy yield and control flexibility, the three-bladed horizontal-axis wind turbine (HAWT) is the most used type of turbine and leads the wind power industry, especially in the high-power segment. However, it has some drawbacks. For instance, turbine rotor and conversion machinery must be installed in a nacelle on the top of a tower of large height involving high logistic costs. Also, the nacelle requires a yaw system that constantly faces the turbine to the incoming wind. For low and

medium-power applications, the vertical-axis wind turbine (VAWT) has recently gained renewed interest from researchers and manufacturers because it does not require a tower or orientation mechanism, and the electric generator is located at ground level, [4], [5]. Among VAWTs, the Darrieus-H appears as the most attractive due to its structural simplicity compared to the traditional Darrieus. Additionally, recent studies have allowed the development of modern design methods, notably increasing its efficiency to around 40%, [6].

Due to the fluctuating nature of the wind resource, one of the main challenges in the wind conversion industry is to enhance power quality by delivering smooth and constant power, [7]. If not, a fluctuating power injected into the grid introduces disturbances that can lead to instabilities of voltage and frequency, and this worsens as the generated power is on the order of the power capacity of the grid (high penetration). Power fluctuations are originated by rapid variations of wind speed which lead to different effects on the conversion chain. Very rapid variations in wind speed generally do not cause serious disturbances as their effect is mitigated by the turbine's inertia. However, changes in wind speed defined as "turbulence" are not fast enough for the turbine's inertia to filter the effect. Therefore, it could produce significant changes in the generator's rotation speed (or torque) leading to variations in the electrical power output of the generator, as well as voltage variations at the point of connection.

One method to mitigate the power fluctuations generated by a turbine due to wind turbulence is using a short-term (low capacity) energy storage system. Among different technologies (supercapacitors, batteries, etc.), the flywheel emerges as one of the most attractive options due to its high power density, high efficiency, and long lifespan, [8], [9]. Particularly, low-speed flywheels are characterized by constructional simplicity, low maintenance, and cost since (unlike high-speed flywheels) they are made using conventional materials, use standard bearings, and do not require a safety container, [10]. A typical flywheel-based power smoothing system consists of a dedicated driving machine with a grid-connected electronic converter. The converter transfers all the flywheel mechanical power to the grid. A control loop adjusts this power to compensate for fluctuations. The machine that moves the flywheel is mechanically separated from the machine that, driven by the wind turbine, acts as a generator.

Electrical Variable Transmissions (EVT) are devices based on electrical machines that allow controlling the transmitted mechanical power between two shafts, which rotate at different speeds, [11]. EVTs are widely used in electric vehicles, [12], but are rarely employed in other applications, exceptions can be seen in [13], [14], [15]. In [13], [14] an EVT is used to couple a variable-speed HAWT with a grid-connected fixed-speed synchronous generator. In [15], a fixed-speed micro-hydro turbine is coupled through an EVT to a variable-speed centrifugal pump for irrigation.

In this work, an EVT is used to integrate both functions: power generation and smoothing in a compact form. A VAWT is coupled to the input shaft of the EVT such that its associated rotor and the stator function as a grid-connected induction generator (fixed-speed "Danish Concept" scheme). The second rotor associated with the output shaft of the EVT, is fed by a variable frequency drive (VFD), which is used as the driving machine of a low-speed flywheel. The flywheel operates at variable speed and is controlled to minimize fluctuations in the power injected into the grid caused by wind turbulence. Thus, an integrated wind energy conversion and power smoothing structure is proposed, specially designed to be used as an RDG system in rural areas with access to electrical utility through a weak grid. Compared to the typical and previously mentioned scheme, the two main advantages of the presented generation/smoothing topology are: (a) the integration of the two machines into a single physical structure resulting in a more compact, simple, and economical system and (b) the electrical power handled by the converter that feeds the flywheel driver is smaller than the one required if it were operated with a separate machine.

2 System Description and Problem Statement

Figure 1 shows a diagram of the proposed wind power conversion system with integrated smoothing capability. It consists of a VAWT, a multiplier gearbox, an EVT, and a low-speed flywheel.

Figure 2 shows the internal structure of the EVT [11]. There is a stator winding, a cup-shaped rotor (rotor 1), and a wound rotor (rotor 2). Shaft 1 drives the cup-shaped rotor which has an inner face and an outer face. The outer face has a squirrel cage, so the stator and the outer face of rotor 1 can be considered as an induction machine. On the other hand, the inner face of rotor 1 has a permanent magnet arrangement which generates a rotating magnetic field around rotor 2. In this way, the machine has

two mechanical ports and two electrical ports, such that electrical and mechanical power can flow from one to the other depending on the electrical excitations of both windings and the relative speeds and torques that are exerted on both shafts.

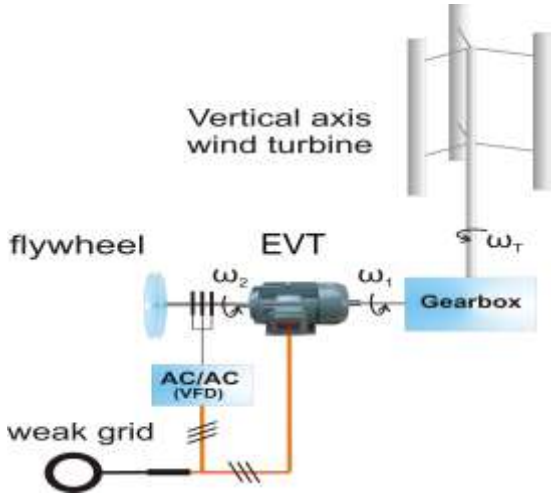

Fig. 1: Integrated generation/smoothing system diagram

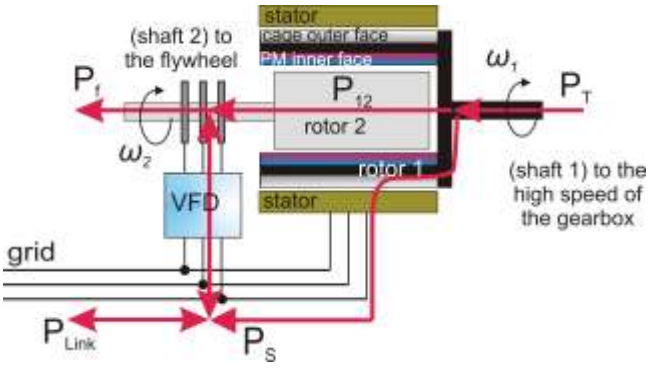

Fig. 2: EVT internal structure

In this proposal, the high-speed shaft of the gearbox is coupled to shaft 1 of the EVT. The stator is directly connected to a weak grid, such that rotor 1 and the stator act as an induction generator. This configuration causes the turbine speed to stay within a small range close to the synchronous speed imposed by the grid frequency. The flywheel is driven by rotor 2 of the EVT whose winding is connected to the output of the VFD, also fed by the grid. The VFD regulates the torque of rotor 2 to establish its idle speed and regulate the power flow between shafts.

2.1 EVT Stator Power Fluctuation Caused by Wind Turbulence

The VAWT is coupled to shaft 1 of the EVT through a multiplier gearbox with a speed ratio a, so that the rotation speed of shaft 1 of the EVT is ω_1:

$$\omega_1 = a\omega_T \tag{1}$$

Where ω_T is the speed of the turbine. The speed ω_1 varies according to Newton's law of rotational dynamics (2):

$$\frac{d\omega_1}{dt} = \frac{1}{J_{T1}}(T_{T1} - T_{em1} - T_{em2}) \tag{2}$$

Where: J_{T1}: Total inertia of shaft 1: $J_{T1} = J_1 + J_T/a^2$ with J_1 inertia moment of rotor 1 and J_T the inertia of the turbine itself. T_{T1}: torque exerted by the turbine referred to shaft 1. T_{em1}: electromagnetic torque between rotor 1 and the stator of the EVT. T_{em2}: electromagnetic torque between rotor 1 and rotor 2 of the EVT.

The torque exerted by the VAWT referred to shaft 1 of EVT is given by (3), [16]:

$$T_{T1} = \frac{1}{a}0.5\rho A R v^2 C_T \tag{3}$$

Where ρ: air density, A: capture area (A=$D.H$, turbine diameter D times height H), v: wind speed and C_T: torque coefficient (depends on ω_1 and v). T_{em1} in (2), is the torque that arises from the interaction of the rotating magnetic field established by the stator winding with the bars of the outer face of rotor 1. Since this part of the EVT configures a traditional induction machine, for T_{em1} to occur, rotor 1 must rotate at a different speed from the magnetic field produced by the stator (there is a slip) which rotates at the synchronous speed ω_s:

$$\omega_s = \frac{2\pi f_{e1}}{p_1} \tag{4}$$

Where f_{e1} is the electrical frequency of the stator, fixed by the grid and p_1 is the number of pole pairs of the stator winding. Considering that rotor 1 operates at a speed close to synchronous speed (low slip), it is possible to calculate T_{em1} through a linear approximation given by (5), [17]:

$$T_{em1} = K_G(\omega_1 - \omega_s) \tag{5}$$

Where K_G is the slope of the torque-speed characteristic whose value depends on the amplitude of the flux in the air gap (determined by the ratio V_s/f_{e1}) and the resistance of rotor bars. Neglecting losses in the stator winding of the EVT, the electrical power injected to the grid (P_s) can be calculated as:

$$P_s = T_{em1}\,\omega_s \tag{6}$$

Taking a time span of less than 10 minutes, the wind speed v reaching the VAWT can be decomposed as a mean value v_o and a turbulence of relatively rapid variation v_t [18]:

$$v = v_0 + v_t \tag{7}$$

Turbulence is random and is mainly caused by ground friction and vertical wind displacement due to thermal heating. The repetition period of turbulence, corresponding to the peak in the high-frequency zone of the Van der Hoven spectrum, is on the order of one minute, [18]. As for the turbulence amplitude, this can be estimated using the IEC61400-2 standard, which provides a Normal Turbulence Model. In many practical cases, it is sufficient to consider that the turbulence intensity is equal to 20% of the mean wind speed, as suggested by DNV GL in 1993, [18].

Although turbulence is a complex phenomenon and cannot be exactly represented by deterministic equations, recent studies propose representing it as a sinusoidal variation to facilitate the analysis, design, and simulation results comparison, [19], [20]. Wind variation can thus be described as (8):

$$v = v_0 + V_t sen\,(2\pi f_t t) \tag{8}$$

Where V_t and f_t are the amplitude and frequency of the equivalent turbulence, respectively.

The torque of the VAWT resulting from introducing (8) into (3) is composed of a constant component and a variable component due to the turbulence. The nonlinear dependence of T_{T1} on v produces harmonics of f_t on the turbine torque but to simplify the system analysis, controller design, and the sizing the flywheel inertia, only the fundamental component is considered here. Therefore, it is assumed that this component exhibits a cosine variation (9):

$$T_{T1} = T_{T10} + T_{T1p} cos(2\pi f_p t) \tag{9}$$

Where T_{T10} is the mean torque, T_{T1p} and f_p are the amplitude and frequency of the torque variation caused by turbulence, respectively.

To analyze power fluctuations on the stator of the EVT using (6), the variation of ω_1 produced by (9) must be evaluated, as T_{em1} depends on ω_1 (5). The relationship between the variable component of T_{T1} and ω_1 is evaluated assuming that $T_{em2}=0$. Then, a transfer function $G_1(s)$ can be derived from (2):

$$G_1(s) = \frac{\omega_1(s)}{T_{T1p}(s)} = \frac{1}{s\,J_{T1}+K_G} \tag{10}$$

$G_1(s)$ has a low-frequency gain $G_{10}=1/K_G$ and exhibits a real pole. This means that the VAWT behaves like an inertial low-pass filter with a cutoff frequency f_1 given by (11):

$$f_1 = \frac{K_G}{2\pi\,J_{T1}} \tag{11}$$

Therefore, the magnitude of the variation of ω_1 caused by T_{T1p} will depend on the relation f_p/f_1. For instance, if $f_p>>f_1$, the variations of ω_1 will be small due to the attenuation produced by the moment of inertia J_{T1}. On the contrary, if $f_p<<f_1$, this attenuation is very small, and then ω_1 can be calculated using G_{10} and (9) as:

$$\omega_1 = \frac{T_{T10}}{K_G} + \frac{T_{T1p}}{K_G} cos\big(2\pi f_p t\big) = \omega_{10} + \omega_{1p} \tag{12}$$

Where ω_{10} is the mean component and ω_{1p} is the variation due to wind turbulence.

If $f_p << f_1$, T_{em1} and T_T are almost equal, as the reaction torque produced by the moment of inertia of the VAWT is very small. Therefore, neglecting second-order terms, the power injected to the grid by the stator of the EVT can be approximated as:

$$P_S = T_{T10}\,\omega_{10} + T_{T1p}\,\omega_{10}\,cos\big(2\pi f_p t\big) = \\ = P_{S0} + P_{Sp} \tag{13}$$

In (13) P_{S0} is the mean power and P_{Sp} the variable power due to the wind turbulence.

3 Compensation of Power Fluctuations

In the previous section, it was assumed that the electromagnetic torque T_{em2} (which arises from the interaction between the field of the permanent magnets located on the inner face of rotor 1 and the winding of rotor 2) has remained null. However, T_{em2} can be adjusted to any desired value through the VFD. Equation (2) indicates that if the VFD is properly managed, it is possible to neutralize the effect that T_{T1p} has over ω_1. If T_{em2} is made equal to:

$$T_{em2p} = T_{T1p} cos(2\pi f_p t) \tag{14}$$

The speed ω_1 will not vary in the presence of the considered turbulence. This means that T_{em1} will not vary either and therefore, P_s will not be disturbed. The drawback of applying (14) is that T_{T1} should be measured, which is costly and complex. However, it is possible to find the appropriate value of T_{em2} if a controller is used to minimize fluctuations in P_s (P_{sp}). P_{sp} is thus obtained by

subtracting the mean value of P_s (P_{so}) obtained, in turn, through low-pass filtering:

$$P_{sp} = P_s - P_{so} \quad (15)$$

Then, T_{em2p} is derived:

$$T_{em2p} = K_C(P_{spref} - P_{sp}) \quad (16)$$

Here K_C is the gain of the controller and P_{spref} is set to 0. To ensure that the flywheel is always capable of absorbing/delivering energy, its idle speed must be set in an intermediate value. Thus, a proportional speed control loop is used (17):

$$T_{em20} = K_{C0}(\omega_{2ref} - \omega_2) \quad (17)$$

Where K_{C0} is the controller gain and ω_{2ref} is the reference speed. It is convenient to set $\omega_{2ref}=\omega_{10}$, the speed of shaft 1 of the EVT corresponding to the mean value of the wind speed. The closed-loop transfer function between ω_2 and T_{em20} has a pole at frequency f_2:

$$f_2 = \frac{K_{C0}}{2\pi\, J_{T2}} \quad (18)$$

Therefore, K_{C0} must be adjusted such that the frequency components of flywheel speed caused by wind turbulence are outside the bandwidth of the idle speed controller, that is $f_2 << f_p$.

Summarizing, to achieve the objectives already mentioned, the reference value T_{em2ref} for the internal torque controller of the VFD should consist of two terms:

$$T_{em2ref} = T_{em2p} + T_{em20} \quad (19)$$

3.1 Sizing of the Flywheel

If the aerodynamic and bearing losses of shaft 2 are negligible, the evolution of the rotation speed of the flywheel is governed by (20):

$$\frac{d\omega_2}{dt} = \frac{1}{J_{T2}} T_{em2} \quad (20)$$

Where $J_{T2}=J_2+J_F$ is the total moment of inertia associated with shaft 2 of the EVT, with J_2 inertia moment of rotor 2 and J_F the inertia of flywheel itself.

If a perfect compensation for P_s is reached, it means that the value of T_{em2} given by (14) is applied and the variations of shaft 1 speed are completely canceled. Under the assumption that initially $\omega_2=\omega_{10}$ (considering an ideal idle speed control loop and that this controller does not provide any corrective action facing a fast speed change), the introduction of (14) into (20) leads to the expression of the instantaneous speed of the flywheel:

$$\omega_2 = \frac{T_{T1p}}{2\pi f_p\ J_{T2}} cos(2\pi f_p t) + \omega_{10} \quad (21)$$

The first term in (21) represents the departure of the flywheel speed concerning the idle speed due to T_{em2p}.

The instantaneous power of the flywheel (p_f) can be obtained by multiplying (14) and (21):

$$p_f = T_{T1p}\ \omega_{10}\ cos(2\pi f_p t) + \\ + \frac{{T_{T1p}}^2}{4\pi f_p\ J_{T2}} sen(4\pi f_p t) = p_{12} + p_{VFD} \quad (22)$$

In (22), the first term (p_{12}) is the power transmitted from shaft 1 to shaft 2 through electromagnetic coupling T_{em2}. The second term corresponds to the power provided by the VFD (p_{VFD}), which has twice the frequency of p_{12}.

It is observed that the proposed compensation technique cancels the power disturbance in the stator of the EVT due to wind turbulence, deriving it to the flywheel through the electromagnetic coupling between both shafts. However, a residual fraction of this disturbance reaches the grid through the VFD. Therefore, an appropriate criterion for sizing the moment of inertia of the flywheel is such that the peak value of the second term in (22) is a small fraction of the peak value of the first term. If we call this fraction K_P:

$$P_{VFDmax} = K_P\ P_{12max} \quad (23)$$

Neglecting J_2 (As $J_F >> J_2$) the required moment of inertia J_F for the flywheel to comply with (23), is:

$$J_F = \frac{P_{12max}}{4\pi f_p\ {\omega_{10}}^2\ K_P} \quad (24)$$

4 Simulation Results

To evaluate the performance of the control scheme for attenuating power fluctuations in the weak grid, a computational model of the system was developed. This model is based on the equations presented in Section 2 in which the main characteristics and parameter values of each part of the model are detailed below.

4.1 VAWT

Three straight-blade Darrieus-H VAWT with a height of H=11.8m and rotation radius of R=10m (capture area A=236m^2), fixed pitch. Nominal power P_T=100kW for a wind speed v=12m/s. The torque coefficient C_T in (3) is calculated with (25):

$$C_T(\lambda,\beta) = \frac{c_1}{\lambda}\left(\frac{c_2}{\lambda_i} - c_3\beta - c_4\right)e^{-\frac{c_5}{\lambda_i}} + c_6 \quad (25)$$

Where λ_i is calculated as (26):

$$\frac{1}{\lambda_i} = \frac{1}{2.25\lambda+0.08\,\beta} - \frac{0.035}{\beta^3+1} \quad (26)$$

In (25) and (26), β is the pitch angle ($\beta=0$ in our case), and $\lambda=(\omega_T R)/v$ is the ratio of the tangential blade speed to the wind speed. The numerical values of the coefficients in (25) are: c_1=0.4332, c_2=116, c_3=0.4, c_4=5, c_5=21, c_6=0.0128. The moment of inertia of the turbine is J_T=52000kgm^2. The turbine is coupled to shaft 1 of the EVT through a speed multiplier gearbox with a ratio of a=38.75. This leads to a rotation speed of shaft 1 of the EVT of 1550RPM for turbine operation in rated conditions.

4.2 EVT

Stator winding: 4 poles, 380V/50Hz, rated power P_N=100kW, synchronous speed n_s=1500RPM. K_G=117.67Nm/(r/s). The rotor of shaft 2 has 4 poles winding, 380V/50Hz, and is fed by a 25kW VFD.

4.3 Flywheel

Using the sizing procedure of Section 2 and adopting K_P=1/5, applying (24) results in J_F=48Kgm^2. Given the low speed of the flywheel, its mechanical and aerodynamic losses are considered negligible.

In a preliminary step, a simulation was conducted to observe how wind turbulence affects the behavior of the VAWT, with the power fluctuation attenuation controller disabled. The results are shown in Figure 3. Figure 3(a) shows the wind speed profile used in the simulations. Starting from a stable wind speed of v=10m/s, after the turbine reached its rated speed, at t=105s, a sinusoidal turbulence with an amplitude of 2m/s appears (representing a turbulence intensity of 20%, [18]). The frequency of turbulence is 16.66mHz, corresponding to the peak of the Van der Hoven spectrum (approximately 1 cycle per minute). In Figure 3(b), the variation of the turbine torque (referred to as shaft 1 of the EVT) is shown, and it is observed that its shape is also sinusoidal with the same frequency as the turbulence, as indicated in Section 2. Using (11), the frequency of the mechanical pole of shaft 1 dynamics can be calculated, resulting in f_1=0.54Hz. Since the frequency of the turbulence is much lower than the pole frequency f_1, nearly all the resulting torque disturbance of Figure 3(b) is directly transferred to the electromagnetic torque T_{em1} (Figure 3(d)). Evidence of this fact is the small value of the torque with which the inertia reacts, Figure 3(c). After the start-up transient, the turbine speed stabilizes, and shaft 1 of the EVT reaches approximately n_1=1525RPM (Figure 3(e)). Due to the steep slope (K_G) of the torque-speed characteristic of the generator composed by the EVT stator and bars on the outer face of rotor 1, the appearance of turbulence causes a very small speed variation around this value, approximately +/-25RPM.

The preliminary simulation confirms that the turbine's inertia has a negligible filtering effect on wind turbulence and the need to add a system to reduce the T_{em1} variations is justified.

This is why the entry into operation of the proposed smoothing system is enabled to attenuate the power fluctuations caused by wind turbulence, and the results are presented in Figure 4, Figure 5 and Figure 6.

In Figure 4, the dynamic behavior of the mechanical variables associated with the flywheel is shown. The flywheel's accelerating/decelerating torque is controlled by the VFD feeding the inner rotor windings. As the dynamic of this loop is determined by short electrical time constants, the torque applied to the flywheel (shaft 2 of the EVT) almost instantaneously copies the torque reference signal. This reference consists of two components: T_{em20} generated by the flywheel's idle speed control loop, and T_{em2p} generated by the control loop for the power smoothing in the EVT stator. Initially, to bring the flywheel into operation, only the slow-speed control loop for idle speed is enabled. This loop has a speed reference n_{2ref} consisting of a step from 0 to 1525RPM at t=50s, as shown in Figure 4(a). A proportional gain K_{Co}=0.3 for the idle speed closed loop is used and produces a torque reference T_{em20} according to (17), which is shown in Figure 4(c). Once the flywheel speed is stabilized (Figure 4(b), t=1025s) the power smoothing loop is enabled. From this moment, the torque reference T_{em2} has an additional component T_{em2p} calculated through (16) with a controller gain K_C=−0.35. This loop produces a T_{em2p} that is sinusoidal with no DC component (Figure 4(d)) resembling the desired torque given in (14) for ideal conditions. T_{em2p} produces fluctuations in the flywheel's speed which varies between 1000 and 2000RPM around its idle speed (Figure 4(b)).

On the other hand, it can be observed that the control loop for the idle speed of the flywheel is indeed slow, presenting a very small gain at the frequency of the turbulence (16.66mHz) since the frequency of the pole f_2 calculated using (18) is 1mHz. Therefore, due to its limited bandwidth, it exerts minimal corrective action when facing rapid speed changes, resulting in a small ripple in T_{em20}, as shown in Figure 4(c). Since mechanical and aerodynamic losses are not considered, the total $T_{em2}=T_{em20}+T_{em2p}$ constitutes flywheel acceleration torque, T_{jf} in Figure 4(e).

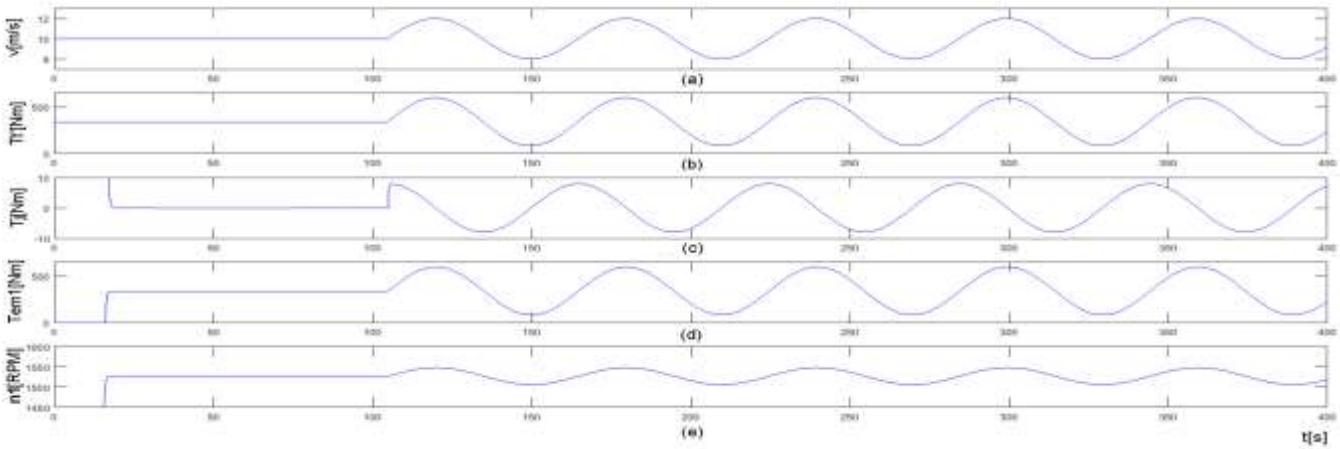

Fig. 3: Effect of wind turbulence on turbine variables (values referred to shaft 1 of the EVT and compensation disabled)

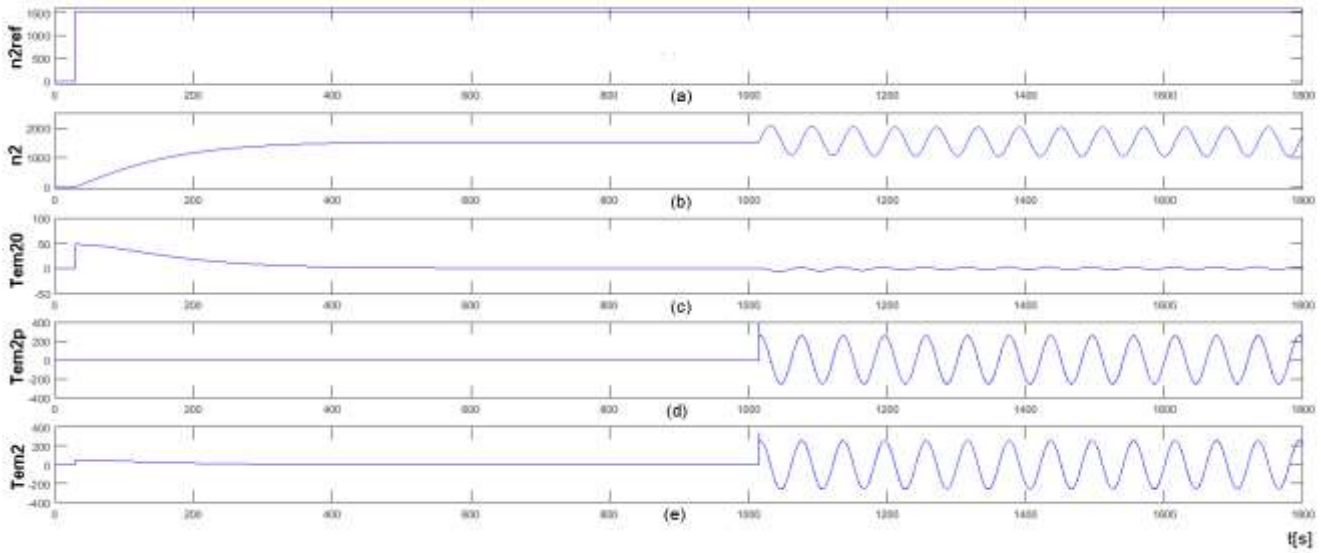

Fig. 4: Mechanical variables of the flywheel (shaft 2 of the EVT and compensation enabled from t=1025s)

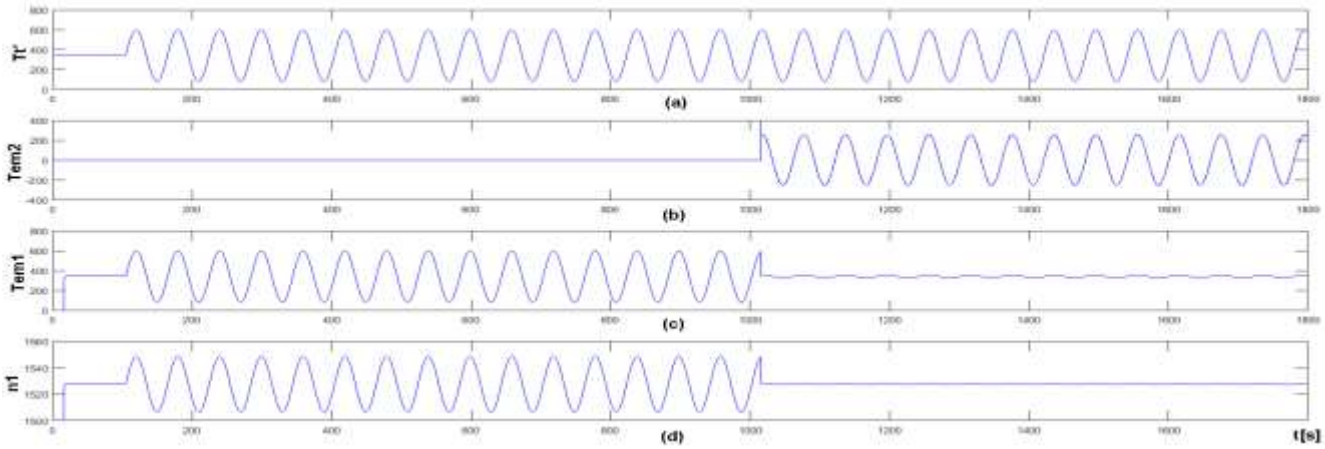

Fig. 5: Mechanical variables on shaft 1 of the EVT (compensation enabled from t=1025s)

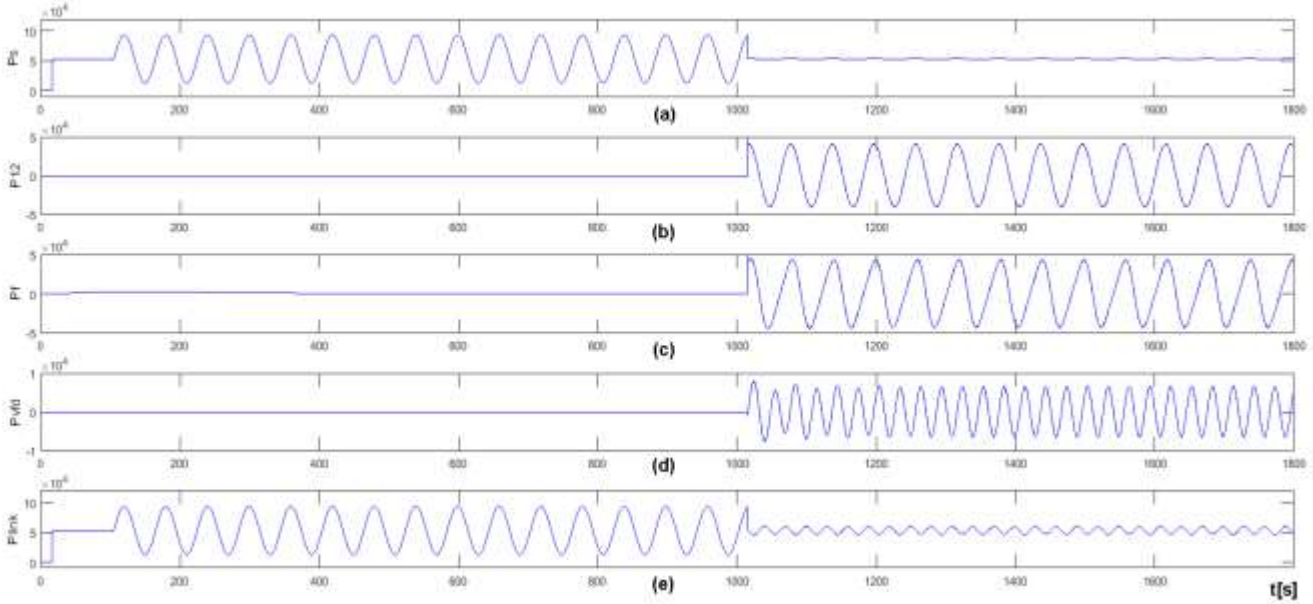

Fig. 6: Power at different points of the system (compensation enabled from t=1025s)

Figure 5 shows the effect on the variables related to shaft 1 of the EVT when the proposed power smoothing system is activated. It can be seen in Figure 5(d), that the speed of shaft 1 (n_1) stops showing significant variations after t=1025s because the variations in turbine torque caused by turbulence (Figure 5(a), referred to as shaft 1 of the EVT) are compensated by equal and opposite variations in T_{em2}, as depicted in Figure 5(b). Since the electromagnetic torque, T_{em1} only depends on the shaft 1 speed, it also ceases to undergo significant variations after t=1025s, as illustrated in Figure 5(c).

In Figure 6, the effect of the smoothing controller on the power at various points of the system is shown. When the controller is enabled (starting from t=1025s), mechanical power is transferred from shaft 1 to shaft 2 through the air gap that exists between the internal face of rotor 1 and rotor 2. This power, P_{12} (Figure 6(b)) is the product of T_{em2} and the rotational speed of rotor 1. As a result, the power in the stator of the EVT, P_s (Figure 6(a)) becomes almost constant from that moment onwards (with a value of around 60kW, corresponding to the average wind speed of 10m/s), as its variations are redirected towards rotor 2 of the EVT. The product of T_{em2} and shaft 2 speed n_2 is the flywheel power P_f (Figure 6(c)). P_f is composed of P_{12} and the power that is managed by the VFD. Neglecting losses in the winding of the inner rotor, the power contributed by the VFD P_{VFD} (Figure 6(d)) can be calculated as the product of T_{em2} and the speed difference between shaft 1 and shaft 2. It is observed that P_{VFD} has twice the frequency of P_{12}. Finally, in Figure 6(e), the power delivered to the weak grid is shown. Before the appearance of turbulence, 60kW corresponding to a constant wind speed of 10m/s is injected. From

t=105s to t=1025s a power fluctuation due to wind turbulence is observed, varying between 20kW to 100kW. This large disturbance in the power (40kW peak value) is injected by the stator of the EVT because the smoothing control system is disabled. Upon enabling the control system, from t=1025s, the initial mean power (60kW) remains unchanged, but the power fluctuation is significantly reduced as the observed new peak value is slightly above 7kW. This corresponds to an attenuation factor of about 5 times, the value that has been adopted in the flywheel sizing stage. This residual power fluctuation is constituted only by the power managed by the VFD, as variations in P_s disappear because are transferred to the flywheel.

5 Conclusions

In this study, we propose a wind energy conversion system that integrates, in a compact form, two functions: power generation and power smoothing. The system has been specifically designed for rural areas in southern Patagonia, Argentina, where challenging environmental conditions and abundant wind resources are prevalent.

The most prominent features of the proposed system are:

- Owing to simplicity and robustness, a VAWT Darrieus-H type has been selected as the wind-to-mechanical energy conversion device.
- A low-speed flywheel is employed as a short-term energy storage device to smooth power fluctuations caused by wind turbulences. This type of flywheel does not require sophisticated materials, special bearings, or a safety container.
- The flywheel is coupled to the VAWT through an EVT.
- The EVT integrates both the generator and the motor to drive the flywheel in a single electrical machine, resulting in a more compact, simple, and economical system than the traditional scheme based on separated machines.
- The chosen EVT is based on induction machines, for reliability and robustness.
- The way the EVT windings are powered and connected is unusual. Only one VFD is required, which is used to feed the inner rotor of the EVT. The stator winding of the EVT is directly connected to the grid. This constitutes a simple and low-cost alternative.
- As a significant fraction of the fluctuating power (generated by the wind turbulence) is transmitted through the electromagnetic coupling between both rotors of the EVT, the VFD-rated power is reduced in comparison with a standard independent flywheel module.
- The proposed control system is straightforward and for its practical implementation a device with low computing power and the measurement of electrical variables are only required. Any simple and commercially available PLC (Programmable Logic Controller) would be more than adequate.

The results of the conducted simulations have been encouraging, showing a significant reduction of the fluctuation in the injected power into the weak grid (around five times in the studied example). Additionally, they validate the theoretical analysis of the system, especially the method for sizing the flywheel to achieve a desired fluctuation attenuation factor.

In future work, an attempt will be made to find an alternative control strategy to achieve a higher level of attenuation of the grid power fluctuation without the need to increase the size of the flywheel. On the other hand, it is planned to use controllers based on advanced techniques which can enhance the system's dynamic performance.

Acknowledgement:
The authors express their gratitude to UNLP, CONICET, CIC, and ANPCyT, since without the support of these institutions, this work would not have been possible.

References:

[1] Q. Tang, J. Wu, J. Xiao, F. Zhou and X. Wu, "A Case Study of Renewable Energy Resources Assessment Results in Argentina", *2021 IEEE 4th International Electrical and Energy Conference (CIEEC)*, Wuhan, China, 2021, pp. 1-5, DOI: 10.1109/CIEEC50170.2021.9510993.

[2] Ruschetti, C., Verucchi, C., Bossio, G., García, G. and Meira, M. (2019), "Design of a wind turbine generator for rural applications". *IET Electric Power Applications*, 13: 379-384, DOI: 10.1049/iet-epa.2018.5734.

[3] Y. Y. Adajah, S. Thomas, M. S. Haruna and S. O. Anaza, "Distributed Generation (DG): A Review," *2021 1st International Conference on Multidisciplinary Engineering and Applied Science (ICMEAS)*, Abuja,

Nigeria, 2021, pp. 1-5, DOI: 10.1109/ICMEAS52683.2021.9692353.

[4] Johari, Muhd Khudri & Jalil, Muhamad & Shariff, Mohammad. (2018). "Comparison of horizontal axis wind turbine (HAWT) and vertical axis wind turbine (VAWT)". *International Journal of Engineering & Technology*, 7 (4.13). 74-80, DOI: 10.14419/ijet.v7i4.13.21333.

[5] Sun, J., Huang, D., "Impact of trailing edge jet on the performance of a vertical axis wind turbine", *Journal of Mechanical Science and Technology*, Vol. 37, No. 3, pp. 1301-1309, 2023, DOI: 10.1007/s12206-023-0216-0, 2023.

[6] Alessandro Bianchini, Giovanni Ferrara, Lorenzo Ferrari, "Design guidelines for H-Darrieus wind turbines: Optimization of the annual energy yield", *Energy Conversion and Management*, Vol. 89, 2015, Pages 690-707, ISSN: 0196-8904, DOI: 10.1016/j.enconman.2014.10.038.

[7] Xing Luo, Jihong Wang, Mark Dooner, Jonathan Clarke, "Overview of current development in electrical energy storage technologies and the application potential in power system operation", *Applied Energy*, Vol.137, pp. 511-536, 2015, DOI: 10.1016/j.apenergy.2014.09.081.

[8] M. Nadour, A. Essadki and T. Nasser, "Power Smoothing Control of DFIG Based Wind Turbine using Flywheel Energy Storage System," *2020 International Conference on Electrical and Information Technologies (ICEIT)*, Rabat, Morocco, 2020, pp. 1-7, DOI: 10.1109/ICEIT48248.2020.9113213.

[9] Andrew Hutchinson, Daniel T. Gladwin, "Optimisation of a wind power site through utilisation of flywheel energy storage technology", *Energy Reports*, Volume 6, Supplement 5, 2020, Pages 259-265, ISSN 2352-4847, DOI: 10.1016/j.egyr.2020.03.032.

[10] R. Sebastián, R. Peña-Alzola, "Control and simulation of a flywheel energy storage for a wind diesel power system", *International Journal of Electrical Power & Energy Systems*, Volume 64, 2015, Pages 1049-1056, ISSN: 0142-0615, DOI: 10.1016/j.ijepes.2014.08.017.

[11] Hoeijmakers, M.J. and Ferreira J.A., ''The Electric Variable Transmission'', *IEEE Trans. on Ind. Appl.*, Vol. 42, no. 4, 2006, pp. 1092–1100, DOI: 10.1109/TIA.2006.877736.

[12] Q. Xu, F. Wang, X. Zhang and S. Cui, "Research on the Efficiency Optimization Control of the Regenerative Braking System of Hybrid Electrical Vehicle Based on Electrical Variable Transmission," in *IEEE Access*, vol. 7, pp. 116823-116834, 2019, DOI: 10.1109/ACCESS.2019.2936370.

[13] Y. Zhu and C. Cai, "Current Source Converter Based Control Strategies for the DPF-WECS", *21st International Conference on Electrical Machines and Systems (ICEMS)*, Jeju, Korea (South), 2018, pp. 1105-1109, DOI: 10.23919/ICEMS.2018.8549187.

[14] X. Sun, M. Cheng, Y. Zhu and L. Xu, "Application of Electrical Variable Transmission in Wind Power Generation System," in *IEEE Transactions on Industry Applications*, vol. 49, no. 3, pp. 1299-1307, May-June 2013, DOI: 10.1109/TIA.2013.2253079.

[15] Marcelo G. Cendoya, Santiago A. Verne, Pedro E. Battaiotto, "Novel Pumping System based on Micro-Hydro Turbine and Centrifugal Pump coupled using EVT Induction Machine. Application in Rural Area Irrigation," *International Journal of Electrical Engineering and Computer Science*, vol. 5, pp. 22-32, 2023, DOI: 10.37394/232027.2023.5.4.

[16] Chen, JS, Chen, Z, Biswas, S, Miau, J, & Hsieh, C. "Torque and Power Coefficients of a Vertical Axis Wind Turbine with Optimal Pitch Control." *Proceedings of the ASME 2010 Power Conference*. Chicago, Illinois, USA. July 13–15, 2010. pp. 655-662, DOI: 10.1115/POWER2010-27224.

[17] B. K. Bose, *Modern Power Electronics and AC Drives 1st Edition*, Pearson Education India, January 2015, ISBN-10: 9332557551.

[18] Burton, T., Jenkins, N., Bossanyi, E., Sharpe, D. & Graham, M., *Wind Energy Handbook 3rd Ed.* John Wiley & Sons Ltd (2021), ISBN: 978-1-119-45109-9.

[19] Wang, X.; Liu, Y.; Wang, L.; Ding, L.; Hu, H. "Numerical Study of Nacelle Wind Speed Characteristics of a Horizontal Axis Wind Turbine under Time-Varying Flow". *Energies* 2019, *12*, 3993, DOI: 10.3390/en12203993.

[20] Lianjun Zhou, Minghui Yin, Xuekun Sun, Dandan Song, "Maximum power point tracking control of wind turbines based on equivalent sinusoidal wind", *Electric Power Systems Research*, Vol. 223, 2023, 109534, ISSN 0378-7796, DOI: 10.1016/j.epsr.2023.109534.

Contribution of Individual Authors to the Creation of a Scientific Article (Ghostwriting Policy)

- Marcelo G. Cendoya has carried out the theoretical analysis of the system. He has developed the mathematical model and has carried out the computer simulations. He has participated in the conception of the system topology. He has collaborated with the writing and revision of the manuscript.
- Santiago Verne has conducted the research on potential advantages of using vertical axis wind turbines in southern Patagonia, Argentina. He has also collaborated in the study of the EVT machine in wind energy conversion applications. He has participated in the conception of the system topology. He did the writing and editing of the manuscript. He has made the figures.
- María Inés Valla has organized and coordinated the tasks that each member of the research group had to perform. She has also carried out the revision and correction of the manuscript.
- Pedro E. Battaiotto has collaborated in the conception of the system topology and the analysis of the EVT operation inside the system. He has also collaborated in the development of the system control scheme.

Sources of Funding for Research Presented in a Scientific Article or Scientific Article Itself

UNLP Proyecto 11/I255 *"Electrónica de Potencia y Sistemas de Control Avanzado Aplicados a Fuentes de Energía Alternativas"*. 1/2020 - 12/2023.

CONICET PIP 112-2020-0102801CO *"Control Avanzado y Electrónica de Potencia Aplicados a la Optimización de Sistemas Basados en Energías No Convencionales"*. 12/2021 – 12/2024.

ANPCyT PICT N°2018-03747 *"Control,*

Conflict of Interest

The authors have no conflicts of interest to declare.